Bulletin of Entomological Research

cambridge.org/ber

Life history and mitochondrial genomes of Salassinae and Agliinae (Insecta, Lepidoptera): New insights into the loss of cocooning behaviour and phylogeny of Saturniidae

Xuhongyi Zheng, Zilong Xu, Dong Wang and Changfa Zhou

The Key Laboratory of Jiangsu Biodiversity and Biotechnology, College of Life Sciences, Nanjing Normal University, Nanjing 210023, China

Research Paper

Cite this article: Zheng X, Xu Z, Wang D, Zhou C (2024). Life history and mitochondrial genomes of Salassinae and Agliinae (Insecta, Lepidoptera): New insights into the loss of cocooning behaviour and phylogeny of Saturniidae. *Bulletin of Entomological Research* **114**, 107–123. https://doi.org/10.1017/S0007485323000676

Received: 21 June 2023
Revised: 9 November 2023
Accepted: 29 November 2023
First published online: 9 January 2024

Keywords:
Aglia; caterpillar; China; *Salassa*; silkmoth

Corresponding author:
Changfa Zhou;
Email: zhouchangfa@njnu.edu.cn

Abstract

The subfamilies Salassinae and Agliinae are two monogeneric groups of the family Saturniidae. They were regarded as the non-cocooning saturniids in Asia. Since very little information on their life history and mitogenome has been reported, their origin and evolution are still poorly understood. In this study, nature-imitated rearing is used to record the life history of two *Aglia* and five *Salassa* species. In addition, four complete mitogenomes are presented, which are the first ones of these two subfamilies. The results show that both Salassinae and Agliinae have lost their cocooning. Moreover, the phylogenetic analysis demonstrates that the subfamily Saturniinae is not monophyletic due to the inclusion of Agliinae and Salassinae.

Introduction

The Saturniidae, also called the giant silkworm, is one of the most eye-catching lepidopteran families. They are usually large and have a great commercial value as ornamental or edible insects (Li *et al.*, 2017). Their cocoons, which are made from silk fibres and sericin binder, are widely used as an important natural polymer composite (Chen *et al.*, 2012). The family comprises many genera and species, and both the larval and adult stages of Saturniidae show much morphological diversity, so that the phylogenetic interpretation of the family is difficult (Friedlander *et al.*, 2002). Nowadays, mitochondrial DNA sequence data are increasingly used to infer saturniid phylogenetic relationships (Chen *et al.*, 2014; Kim *et al.*, 2018; Rubinoff and Doorenweerd, 2020). However, sequences of Asian species are still scarce, which greatly hindered further research (Chen *et al.*, 2022; Lu *et al.*, 2022; Nethavhani *et al.*, 2022).

Within the Bombycoidea spinning behaviour is regarded as a plesiomorphic behaviour of Saturniidae (Chen *et al.*, 2012; Tsukada *et al.*, 2012). In other Bombycoidea, such as the Sphingidae, the spinning behaviour is degenerated or completely lost, and is replaced by an underground-pupation stage (Lampe, 2010). This loss of spinning behaviour in different taxa has not been studied systematically. Most of the non-cocooning saturniid groups were reported from Africa, and only species of *Salassa* and *Aglia* were reported to be non-cocooning in Asia (Lampe, 2010). Hence to explore the evolution of spinning behaviour (cocooning), more mitogenomic evidence of non-cocooning saturniids is needed, particularly from Asian taxa.

Agliinae and Salassinae are two monogeneric subfamilies of Saturniidae whose life histories and mitogenomes are still poorly known (Regier *et al.*, 2008). The genus *Aglia* Ochsenheimer, 1810 has a Palaearctic distribution, whereas the genus *Salassa* Moore, 1859 is distributed in both the Palaearctic and Oriental realms (Lampe, 2010). The life histories of only one *Aglia* and two *Salassa* species have been reported (Lampe, 2010). Yet, although the pupation process in these two genera has not been described or studied in detail, *Aglia* and *Salassa* species appear to be non-cocooning under indoor rearing conditions (Lampe, 2010). Hence Agliinae and Salassinae are possibly the only non-cocooning Saturniidae in Asia. However, whether non-cocooning is a natural and universal behaviour in these two subfamilies requires further confirmation.

Against this background, the present study reports for the first time on the successful indoor rearing of several *Aglia* and *Salassa* species. Pupation behaviour of two *Aglia* and five *Salassa* species was observed, and mitogenomes of both genera were sequenced for the first time. Combining these mitogenomic and behavioural data may help to trace the evolutionary gain and loss of cocooning behaviour in the phylogenetic framework of the Saturniidae.

Materials and methods

Collection, rearing and observation of saturniid species

Specimens used in this study were collected in China between 2021 and 2022. Eggs of *Aglia tau* (Linnaeus, 1758), *Aglia homora* Jordan, 1911, *Salassa shuyiae* Zhang and Kohll, 2008,

Salassa mesosa Jordan, 1910, *Salassa paratonkiniana* Brechlin, 2009, *Salassa daxuensis* Brechlin, 2015 and *Salassa arianae* Brechlin & Kitching, 2010 were obtained from wild-caught adult females through light traps.

Larvae were reared and observed in mesh cages inside a room, where temperature was controlled by an air conditioner. Food of larvae was replaced every two days before the leaves dried. To observe their natural pupation behaviour, mature larvae were moved to large tree branches inserted in pots with soft soil and moss.

Sample identification and DNA extraction

The morphological identification was mainly based on Naumann and Lalhmingliani (2019) and Naumann, Brosch and Nässig (2003). All samples were preserved in 85% ethanol, and stored

Table 1. GenBank accession numbers of mitogenome sequences of species used in this study with references on their life history and cocooning behaviour

Family	Genus	Species	GenBank ID	References
Saturniidae	*Aglia*	*Aglia homora*	OQ786760 (this study)	Lampe, 2010; Poulton, 1888
		Aglia tau	OQ786761 (this study)	
	Salassa	*Salassa shuyiae*	OQ786762 (this study)	Lampe (2010)
		Salassa mesosa	OQ786763 (this study)	
	Actias	*Actias maenas*	MG836834.1	Lampe (2010)
		Actias dubernardi	MW133617.1	
		Actias selene	JX186589.1	
	Antheraea	*Antheraea assama*	KU301792.1	Lampe (2010)
		Antheraea pernyi	MN064713.1	
		Antheraea yamamai	MW009051.1	
	Attacus	*Attacus atlas*	KF006326.1	Lampe (2010)
	Bunaea	*Bunaea alcinoe*	OL912807.1	Lampe, 2010; Taylor, 1964
	Cricula	*Cricula Andrei*	OM236670.1	Lampe (2010)
	Eochroa	*Eochroa trimenii*	OL912808.1	Lampe, 2010; Rougerie and Estradel 2008
	Epiphora	*Epiphora bauhiniae*	OL912809.1	Lampe, 2010; Eltayba and Magidb, 2013
	Gonimbrasia	*Gonimbrasia belina*	MN832538.1	Lampe (2010)
		Gonimbrasia cytherea	OL912953.1	
		Gonimbrasia tyrrhea	OL912810.1	
	Gynanisa	*Gynanisa maja*	MN832541.1	Lampe (2010)
	Heniocha	*Heniocha apollonian*	OL912811.1	Lampe (2010)
		Heniocha dyops	OL912812.1	
	Holocerina	*Holocerina smilax*	OL912813.1	Lampe (2010)
	Imbrasia	*Imbrasia wahlbergi*	OL912817.1	Lampe (2010)
	Ludia	*Ludia delegorguei*	OL912814.1	Lampe (2010)
	Neoris	*Neoris haraldi*	MF664471.1	Lampe, 2010; Zhang, Yue, Liu and Ma, 2011
	Rhodinia	*Rhodinia fugax*	MT548575.1	Lampe (2010)
	Samia	*Samia canningi*	KJ159909.1	Lampe, 2010; Peigler and Liu, 2022
		Samia cynthia	KC812618.1	
		Samia wangi	ON080860.1	
	Saturnia	*Saturnia pyretorum*	FJ685653.1	Lampe, 2010; Liu and Peigler, 2021
		Saturnia boisduvalii	MF034742.1	
		Saturnia japonica	MT614593.1	
	Vegetia	*Vegetia ducalis*	OL912815.1	Lampe, 2010; Oberprieler, Morton and van Noort, 2021
		Vegetia grimmia	OL912816.1	
Lasiocampidae	*Trabala*	*Trabala vishnou*	MZ927091.1	
Brahmaeidae	*Brahmaea*	*Brahmaea hearseyi*	KU884326.1	
Bombycidae	*Andraca*	*Andraca olivacea*	MF100135.1	

https://doi.org/10.1017/S0007485323000676 Published online by Cambridge University Press

at −20°C in the Lepidoptera Collection of Nanjing Normal University. Genomic DNA was extracted from muscle tissue of each species using the TIANamp Genomic DNA Kit (TIANGEN, Beijing, China). DNA concentrations were determined by a Nanodrop 2000 spectrophotometer.

Mitogenome sequencing and assembly

DNA was sequenced using next-generation sequencing (NGS) on the Illumina NovaSeq platform. The library of each sample was constructed by TruSeqTM DNA Sample Prep Kit (insert size 400 bp). All libraries were sequenced based on the PE150 mode (paired-end, 2 × 150 bp). Around 4 GB of raw data from each sample were trimmed so that adaptor contamination, and short and low-quality reads were removed using Fastp (Chen *et al.*, 2018). MitoZ was used for the assembly of the mitogenomes (Meng *et al.*, 2019), with the kmers-megahit = 79, 99, 119, 141. To verify the accuracy of NGS sequencing results, *COI* gene fragments of all samples were sequenced using Sanger sequencing with the primer pair (LCO1490 as a forward primer, 5'-GGTCAACAAATCATAAAGATATTGG-3'; HCO2198 as a reverse primer, 5'-TAAACTTCAGGGTGACCAAAAAATCA-3') (Folmer *et al.*, 1994). r-Taq polymerase (Takara, Beijing, China) was used for the polymerase chain reaction based on the method of Yanai *et al.* (2017).

Mitogenome annotation and analysis

The mitogenomes were annotated using the MITOS WebServer (Bernt *et al.*, 2013) and MitoZ (Meng *et al.*, 2019) and aligned with available sequences of *Ephemera* from GenBank using ClustalW in MEGA 11 (Tamura, Stecher and Kumar, 2021). The secondary structures of tRNAs were determined using tRNAscanSE 2.0 (Lowe and Chan, 2016) and the MITOS WebServer (Bernt *et al.*, 2013). The circular mitogenome maps were portrayed using the visualisation module of MitoZ (Meng *et al.*, 2019).

Four newly sequenced mitogenomes, viz. *Aglia tau* (Linnaeus, 1758), *Aglia homora* Jordan, 1911, *Salassa shuyiae* Zhang and Kohll, 2008 and *Salassa mesosa* Jordan, 1910 (table 1) were used in the comparative analysis. Nucleotide composition and relative synonymous codon usage were assessed with MEGA11 (Tamura, Stecher and Kumar, 2021). The AT-skew and GC-skew were calculated by the formulas: AT-skew = (A − T)/(A + T) and GC-skew = (G − C) / (G + C) (Perna and Kocher, 1995). A sliding window analysis of 200

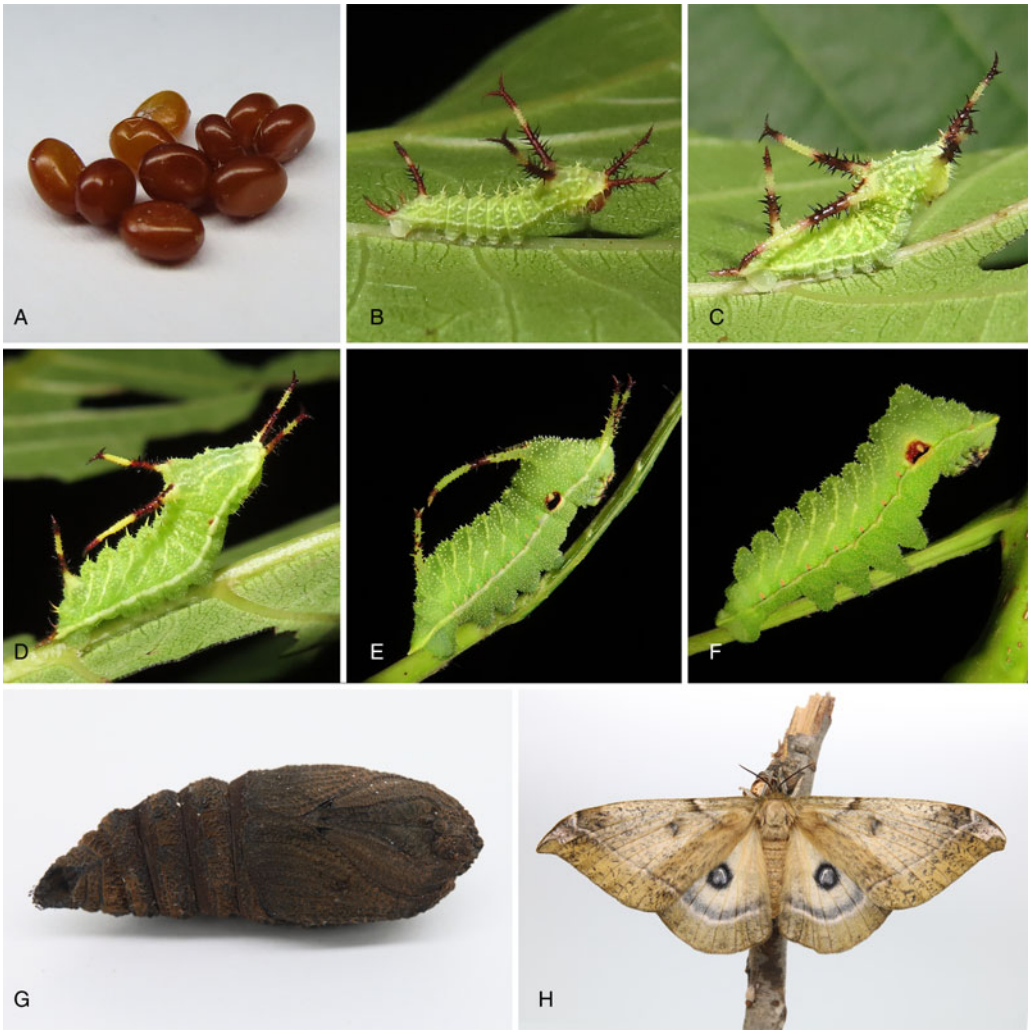

Figure 1. Life history of *Aglia homora*. (**A**) eggs. (**B**) L1 larva. (**C**) L2 larva. (**D**) L3 larva. (**E**) L4 larva. (**F**) L5 larva. (**G**) pupa. (**H**) female adult.

https://doi.org/10.1017/S0007485323000676 Published online by Cambridge University Press

bp (step size 20 bp) was used to estimate nucleotide diversity (Pi) of 13 PCGs by DnaSP V6 (Rozas *et al.*, 2017). K2P distances (Kimura, 1980) of the mitogenomes were estimated using MEGA11. The ratio of nonsynonymous/synonymous (Ka/Ks) substitution rates of 13 PCGs was calculated by DnaSP V6 (Rozas *et al.*, 2017).

Phylogenetic analysis

A total of 37 mitogenomes of four families were used for the phylogenetic reconstruction, including 34 species of 20 genera within Saturniidae as ingroup, and three species from three families as outgroup (Table 1).

The nucleotide sequences of 13 PCGs were aligned with MAFFT (Katoh and Standley, 2013) L-INS-i (accurate) strategy and codon alignment mode in PhyloSuite v1.2.2 (Zhang *et al.*, 2020). The ambiguous sites were removed using Gblocks 0.91b (Talavera and Castresana, 2007). Individual genes were then concatenated using PhyloSuite v1.2.2 (Zhang *et al.*, 2020). The PCGs matrix, with all codon positions of the 13 protein-coding genes was used for the reconstruction of the phylogenetic relationships. For the phylogenetic reconstruction, Bayesian inference (BI) and maximum likelihood (ML) analyses were performed. The partition model of each dataset was selected by the ModelFinder based on Bayesian information criterion (BIC) and AICc (standard correction to Akaike information criterion) (Kalyaanamoorthy *et al.*, 2017). BI phylogenies were reconstructed using MrBayes 3.2.6 through the online CIPRES Science Gateway (Miller, Wayne and Terri, 2011; Ronquist *et al.*, 2012), with the following settings: two parallel runs with four Markov chains were run for 10 million generations (with a sample frequency of 1000), with a burn-in of 25% trees. RAxML 8.2.0 was used for ML analysis with the GTR + Γ + I model and 1000 bootstrap replicates (Stamatakis, 2014). FigTree 1.4.2 (http://tree.bio.ed.ac.uk/software/figtree/; accessed on 5 July 2021) was used for the editing of phylogenetic trees.

Results

Life history of Aglia homora *Jordan, 1911*

Three host plants were used, viz. *Juglans regia*, *Quercus glandulifera* and *Salix babylonica*.

Eggs were obtained from wild adult females caught in China: Taibai Mountain, Baoji City, Shaanxi Province, 1000 m a.s.l., 19-V-2021.

Eggs were amber in colour (fig. 1A). L1 larva light green, body covered with small light yellowish thorns and with six long spiny

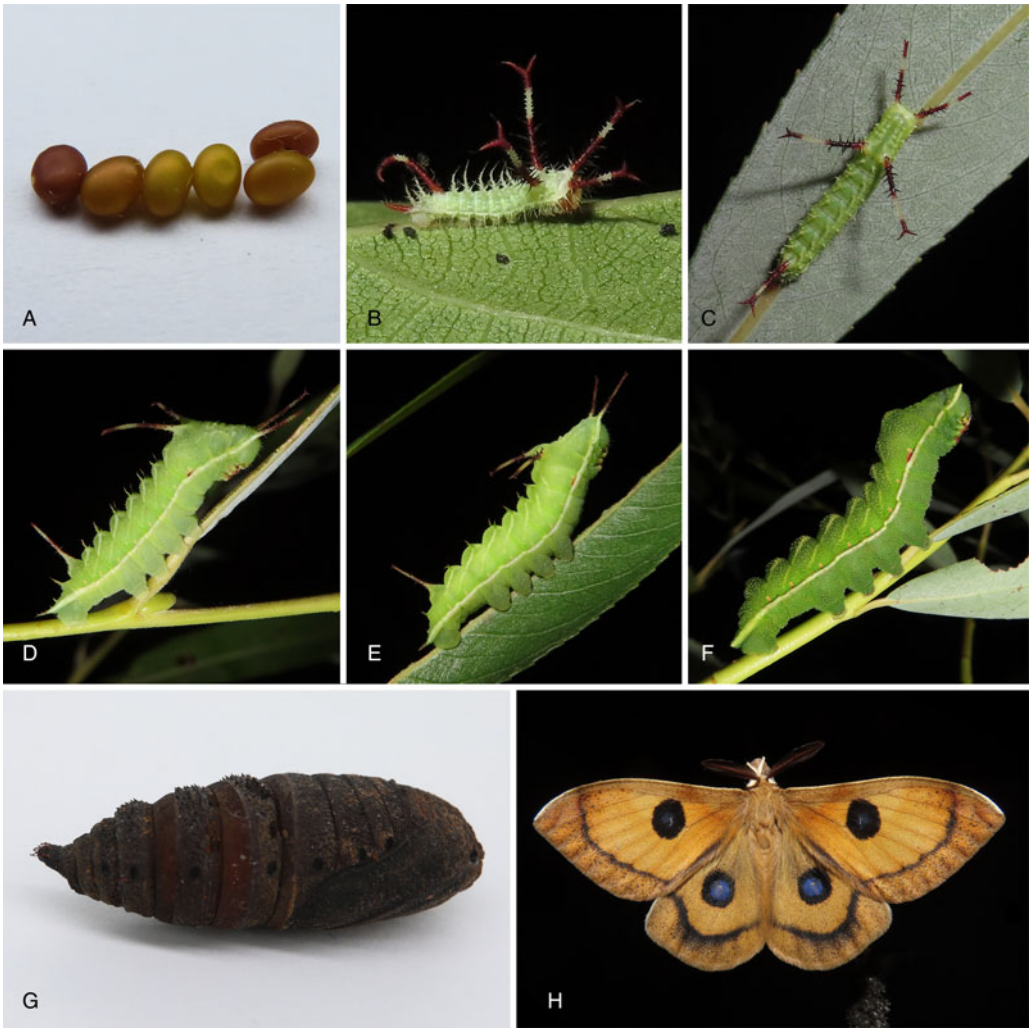

Figure 2. Life history of *Aglia tau*. (**A**) eggs. (**B**) L1 larva. (**C**) L2 larva. (**D**) L3 larva. (**E**) L4 larva. (**F**) L5 larva. (**G**) pupa. (**H**) male adult.

https://doi.org/10.1017/S0007485323000676 Published online by Cambridge University Press

thorns: one pair right behind the head, pointing forward, bifurcated apically; one pair slightly behind the anterior pair, longest amongst the six ones, pointing backward, bifurcated apically; one near the posterior end, bifurcated apically, pointing upward, and one located at the posterior end, shortest amongst the six, pointing backward (fig. 1B). Except for the shortest posterior thorn which is totally reddish, the other five thorns are reddish brown apically and basally, light-yellowish medially (fig. 1B). L2 larva generally similar to L1, but with several oblique white lines dorsally on abdomen, body surrounded by a circular white line on lateral margin; shape and colour pattern of the six long thorns same as L1 (fig. 1C). L3 larva similar to L2, but with a pair of red dots on lateral margin below the second pair of thorns (fig. 1D). L4 larva without small light yellowish thorns on the abdomen, but with white tubercles all over the body. There are only five, instead of six, long thorns, which are green with apical and median red dots. The lateral red dot in L3 becomes an eyespot in L4 larva (fig. 1E). L5 larva without thorns, lateral eyespots larger, body covered with tiny white tubercles, body colour turned reddish from green when fully matured before pupation (fig. 1F). Pupae brownish black, darker at high humidity, yellowish brown at low humidity; abdominal segments V–VII with a patch of dorsal spines (fig. 1G). Adult morphology: see original description (fig. 1H).

Of the three host plant species studied, *J. regia* is the most successful with a larval survival rate above 50%, larvae pupate in 30–35 days after hatching and are on average larger than on other host plants. Larvae that feed on *S. babylonica* have a survival rate of ca. 50%, pupate in 40–50 days after hatching and remain on average smaller than larvae feeding on *J. regia*. Although several larvae that fed on *Q. glandulifera* completed their life cycle successfully, their survival rate was less than 10%, their larval stage lasted more than 100 days, and their pupae remained smaller. Overall, larvae did not aggregate together, but clearly preferred tender leaves and avoided old leaves. To simulate the natural temperature conditions, pupae were kept at 5°C from September 2021 to March 2022, after which they were kept at 15–20°C. With this latter temperature regime adults emerged within 25–35 days.

Life history of Aglia tau *(Linnaeus, 1758)*

Three host plants were used, viz. *J. regia*, *Q. glandulifera* and *S. babylonica*.

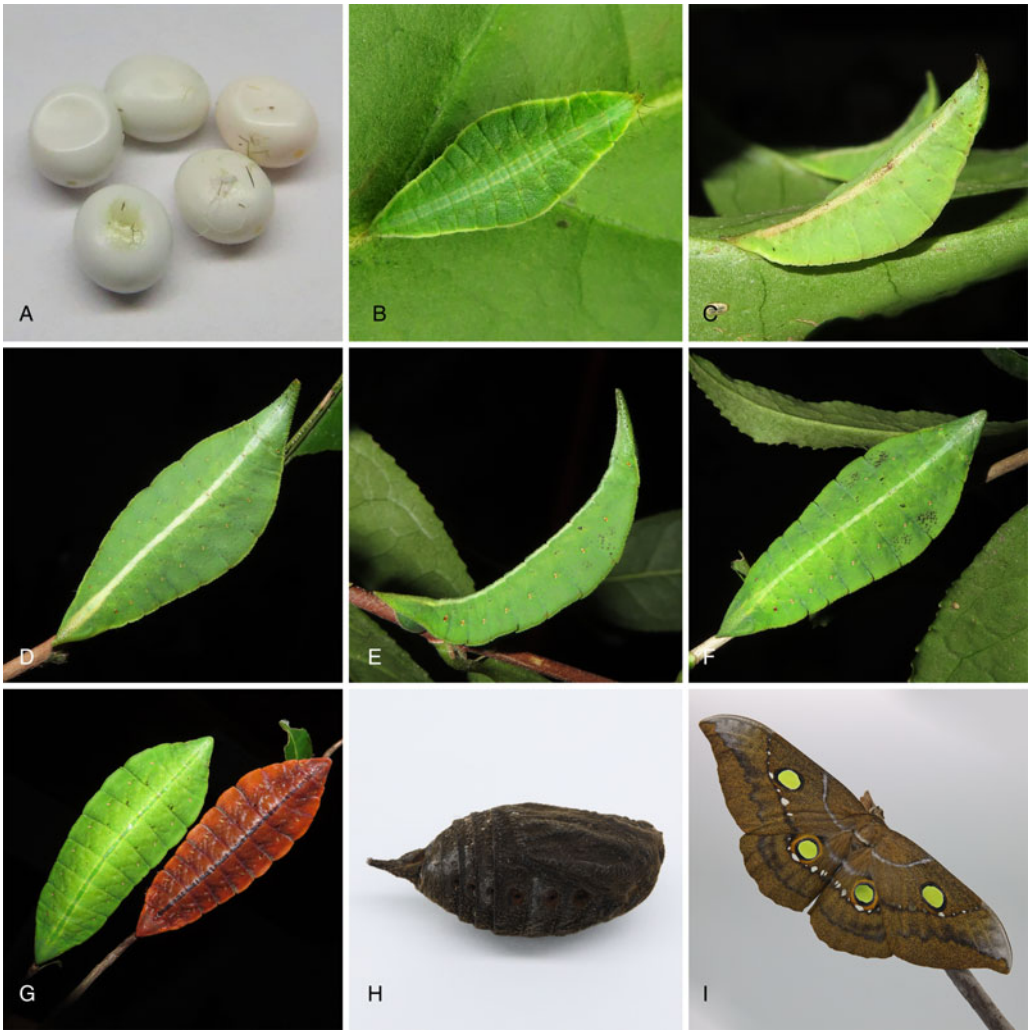

Figure 3. Life history of *Salassa shuyiae*. (**A**) eggs. (**B**) L1 larva. (**C**) L2 larva. (**D**) L3 larva. (**E**) L4 larva. (**F**) L5 larva. (**G**) L6 larva. (**H**) pupa. (**I**) female adult.

https://doi.org/10.1017/S0007485323000676 Published online by Cambridge University Press

Eggs were obtained from wild adult females caught in China: Suiyang Town, Dongning City, Mudanjiang City, Heilongjiang Province, 600 m a.s.l., 24-V-2021.

Eggs were amber in colour (fig. 2A). L1 larva light green, body covered with multiple paired light yellowish thorns and with six long spiny thorns: one pair right behind the head, pointing forward; one pair, involving the longest thorns, slightly behind the anterior pair, pointing backward; one thorn near the posterior end and pointing upward; and finally, one thorn, i.e. the shortest one of the six, located at the posterior end and pointing backward (fig. 2B). Except for the shortest posterior thorn which is totally reddish and non-bifurcated, the other five thorns are apically bifurcated and share a similar colour pattern, viz. reddish brown apically and basally, light-yellowish medially (fig. 2B). L2 larva generally similar to L1, but with several oblique white dorsal lines on the abdomen and a circular white line surrounding the body. The shape and colour pattern of the six long thorns is the same as in L1 (fig. 2C). L3 larva similar to L4, body covered with tiny white dots, a pair of white dorsal thorns present on each abdominal segment. The six long thorns are relatively shorter in instars; lateral margin below the second pair of thorns with two red dots (fig. 2D, E). L5 larva without thorns, body covered with tiny white tubercles, the entire body turned reddish from green when fully matured before pupation (fig. 2F). Larval morphology similar to *A. homora*, but with thinner thorns, L4 and L5 larvae with smaller dots below the second pair of thorns. Pupae brownish black, darker at high humidity, yellowish brown at low humidity; abdominal segments V–VII with a patch of dorsal spines (fig. 2G). Adult morphology see original description (fig. 2H).

Of the four host plants studied, *J. regia* is the most successful, with a larval survival rate of ca. 80%, larvae pupate in 25–35 days after hatching and larvae are on average larger than on other host plants. Larvae fed on *S. babylonica* have a survival rate of ca. 50%, pupate 40–50 days after hatching, and are on average smaller than larvae fed on *J. regia*. Larvae fed on *Q. glandulifera* have a survival rate of ca. 50%, need at least 80 days to reach pupation time, and yield pupae that are smaller than on the other host plants. Finally, larvae fed on *Acer truncatum* all died in the L1 or L2 stage. Larval behaviour similar to *A. homora*. To simulate the natural temperature conditions, pupae were kept at 5°C from September 2021 to March 2022, after which they were kept at 15–20°C. With this latter temperature regime adults emerged within 14–20 days.

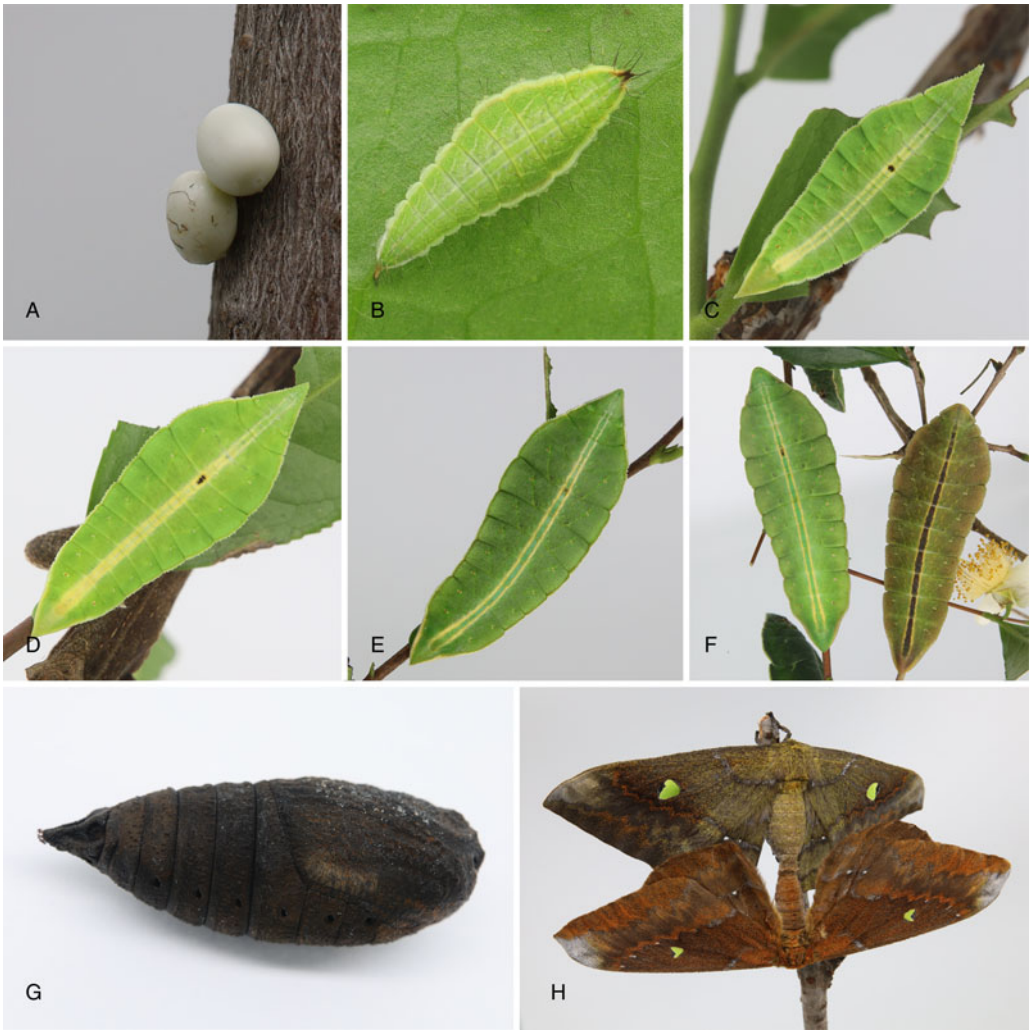

Figure 4. Life history of *Salassa mesosa*. (**A**) eggs. (**B**) L1 larva. (**C**) L2 larva. (**D**) L3 larva. (**E**) L4 larva. (**F**) L5 larva. (**G**) pupa. (**H**) mating adults.

https://doi.org/10.1017/S0007485323000676 Published online by Cambridge University Press

Life history of Salassa shuyiae *Zhang and Kohll, 2008*

Two host plants were used, viz. *Camellia sinensis* and *Litsea pungens*.

Eggs were obtained from wild adult females caught in China: Bawang Mountain, Changjiang Li Autonomous County, Hainan Province, 600 m a.s.l., 15-XI-2021.

Eggs white, oblate (fig. 3A). L1 larva green, flat, leaf-shaped in dorsal view; body margin marked by a light yellowish line and black setae. Such setae also occur along the midline; midline consists of a green band between a pair of white lines; head and posterior end sharp, with a light brownish apex (fig. 3B). L2 larva without setae and obvious light yellowish line on lateral margin; head, caudal region and midline densely covered with tiny tubercles; midline consists of a white band; near the midline at the posterior margin of each abdominal segment there are 1–3 black dots; head slender triangular shaped and curved upward, both head and posterior end with a sharp apex, light brownish apically (fig. 3C). L3, L4, and L5 larva generally similar to L2 larva (fig. 3D–F); except larger body, L4 and L5 larva have a large patch of black dots near the lateral margin of several medial abdominal segments (fig. 3E, F). The L5 larva has a relatively short head (fig. 3F). In the L6 larva the midline consists of a green band between a pair of white lines; head shaped as an equilateral triangle in dorsal view; both head and posterior end blunt (fig. 3G). When L6 larvae reach maturity, they change colour from green to red (fig. 3G). Pupae brownish black, darker at high humidity; yellowish brown at low humidity, terminal segment sharp and slender (fig. 3H). Adult morphology see original description (fig. 3I).

Eggs kept at 10–13°C, hatched within 45 days, in the period 20–28 December 2021. Hatching could be stimulated by water, mature eggs hatched within two hours after watering, keeping dry can delay the hatching process and increase failure rates. Seven host plants were used in this study. Amongst them, *C. sinensis* and *L. pungens* yielded similar results, with a survival rate above 50% until pupation. Yet, larvae feeding on *L. pungens* become slightly larger than larvae feeding on *C. sinensis*. Larvae reared at 17–20°C, instars I–VI last for ca. 10, 11, 11, 12, 20, and 30 days respectively. We also experimented with *Ligustrum compactum*, *Ilex chinensis*, *C. sinensis,* and *Deyeuxia langsdorffii*, all the larvae died before L2. During this study, larvae showed no aggregation behaviour, smaller larvae usually rest under leaves at the main vein, larger larvae rest on the branches. Pupae were kept in 25–30°C, watered once a week. Adults emerged after ca. 130 days, but only 10% emerged successfully, 70% got out of the pupae but did not unfold their wings, 20% died in pupae. This may have been caused by inappropriate temperature and humidity conditions.

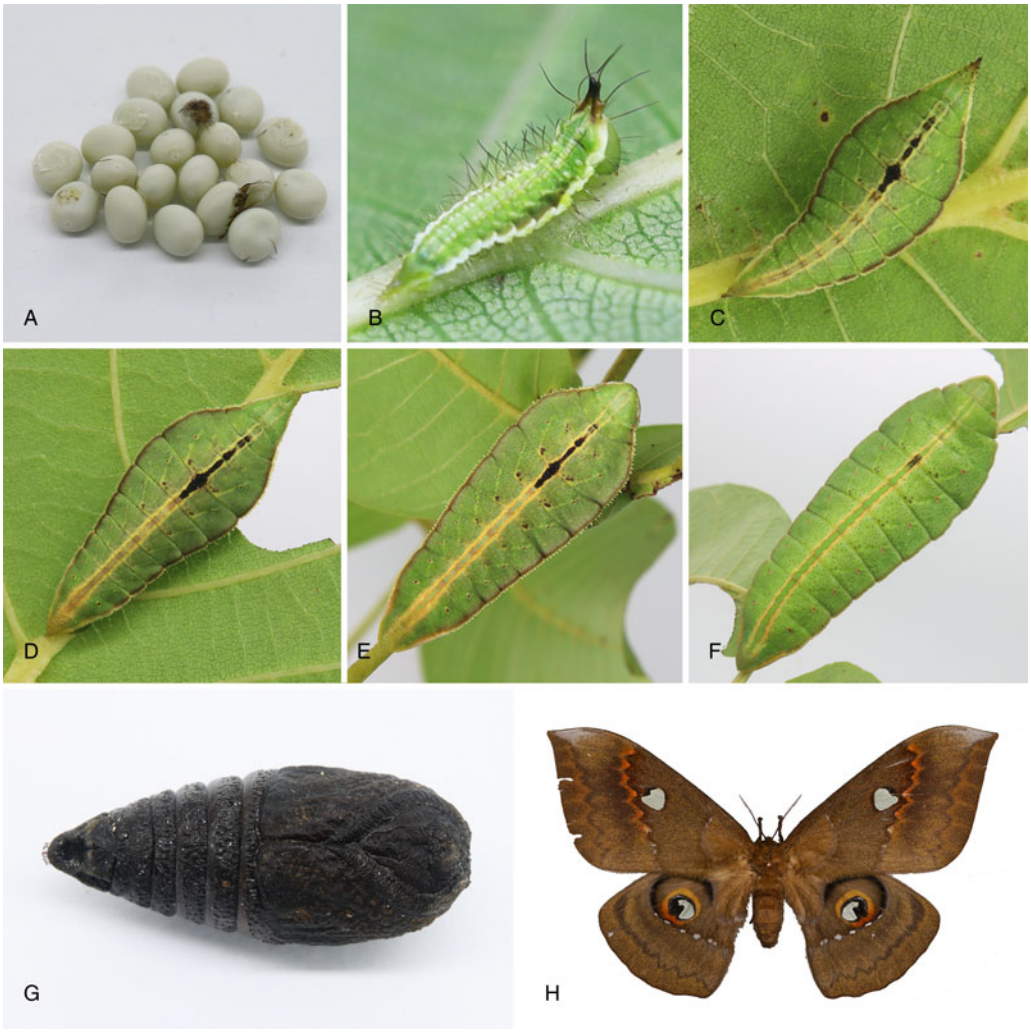

Figure 5. Life history of *Salassa paratonkiniana*. (**A**) eggs. (**B**) L1 larva. (**C**) L2 larva. (**D**) L3 larva. (**E**) L4 larva. (**F**) L5 larva. (**G**) pupa. (**H**) female adult.

https://doi.org/10.1017/S0007485323000676 Published online by Cambridge University Press

Life history of Salassa mesosa *Jordan, 1910*

Three host plants were used, viz. *C. sinensis*, *J. regia* and *L. pungens*.

Eggs were obtained from wild adult female caught in China: Gulinqing, Maguan County, Wenshan Prefecture, Yunnan Province, 1200 m a.s.l., 31-VIII-2022.

Eggs white, oblate (fig. 4A). L1 larva similar to *S. shuyiae*, but body margin marked by a wider light yellowish line, head light brownish and bifurcated apically (fig. 4B). Compared with *S. shuyiae*, L2 larvae of *S. mesosa* with shorter head, which is slender triangular shaped with a sharp apex, body midline consists of a green band between a pair of white lines, lateral margin covered with small white denticles (fig. 4C); L3, L4, and L5 larvae generally similar to L2 larva (fig. 4D–F); except that they are larger, the light yellow margin gradually narrower in later instars, head of L3 and L4 larvae shortened into an equilateral triangle in dorsal view, but rounded in L5 (fig. 4D–F). Body colour darker in L5 larva, changing from dark green to brownish when fully matured before pupation (fig. 4F). Pupae brownish black, darker at high humidity, yellowish brown at low humidity (fig. 4G). Adult morphology see original description (fig. 4H).

Eggs kept at 20°C hatched within 15 days. Hatching process and larval behaviour similar to *S. shuyiae*. Of the three host plants used in this study, *C. sinensis* and *L. pungens* yielded similar results, viz. larvae pupate within 55 days with a survival above 70% until pupation. Larvae fed on *J. regia* pupate within 60 days with a survival rate of ca. 35%. We also tried *Lindera glauca* as host plant, but all the larvae died in L2. All the larvae pupated in December 2022. Next, the pupae were kept at 8°C for 90 days and watered once a week. Adults emerged in February 2023, with a success rate of 90%.

Life history of Salassa paratonkiniana *Brechlin, 2009*

Host plant: *Juglans regia*.

Eggs were obtained from wild adult females caught in China: Shimen Gorge, Ailao Mountain, Yuxi City, Yunnan Province, 2200 m a.s.l., 6-VII-2022.

Eggs white, oblate (fig. 5A). L1 similar to *S. mesosa* (fig. 5B). L2 larva distinguishable from *S. mesosa* through a black band just before the centre of body midline, and lateral margin marked by a purplish brown line (fig. 5C). L3 larva generally similar to L2 larva except for its larger body size (fig. 5D). The head of L4 and L5 larvae is shortened and rounded apically (fig. 5E, F). Their body colour changes from green to brownish when fully matured before pupation. Pupae brownish black, darker at high

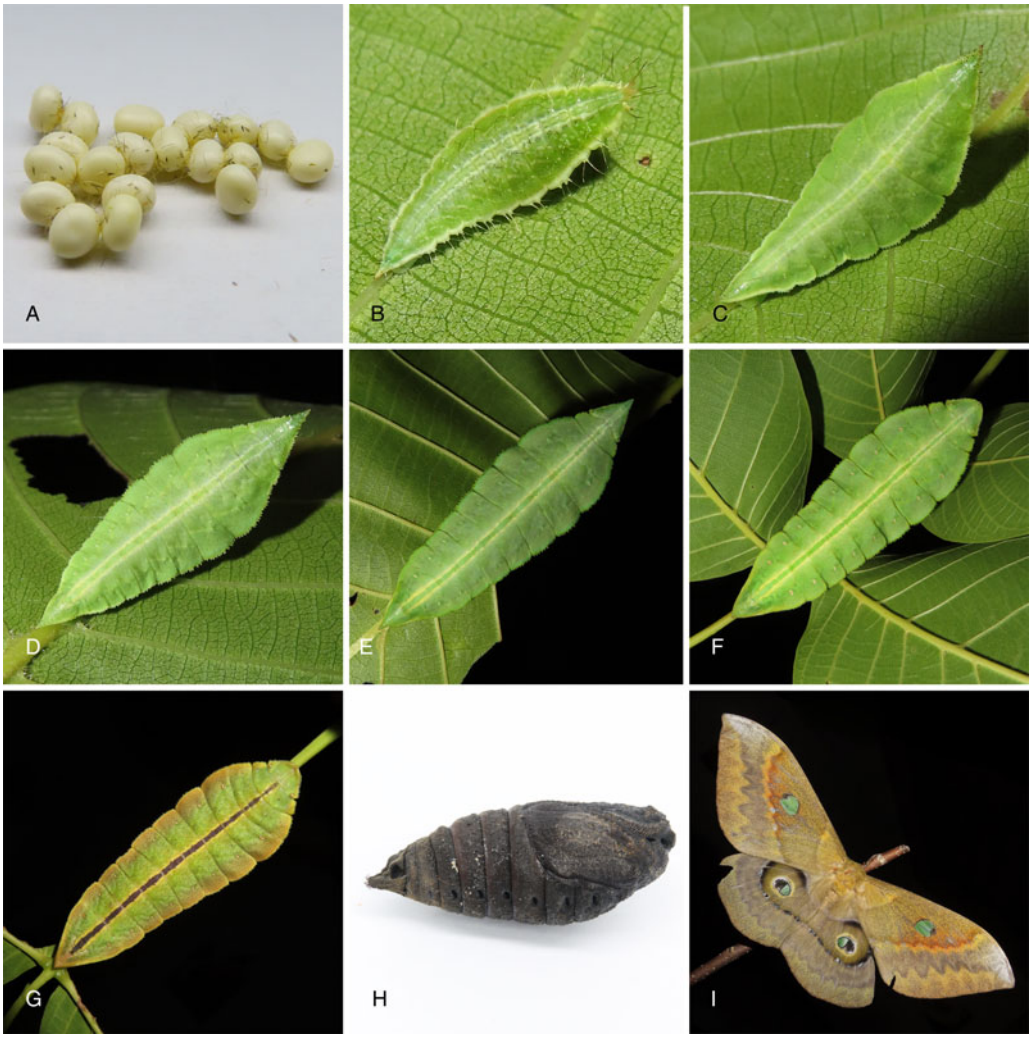

Figure 6. Life history of *Salassa daxuensis*. (**A**) eggs. (**B**) L1 larva. (**C**) L2 larva. (**D**) L3 larva. (**E**) L4 larva. (**F**) L5 larva. (**G**) L6 larva. (**H**) pupa. (**I**) female adult.

https://doi.org/10.1017/S0007485323000676 Published online by Cambridge University Press

humidity, yellowish brown at low humidity (fig. 5G). Adult morphology see original description (fig. 5H).

Eggs kept at 20°C, hatched within 15 days. Hatching process and larval behaviour similar to *S. shuyiae*. Larval survival rate was ca. 30%, and larvae pupated within 75 days. The larval colour patterns is far more variable than in the other species in this study. Pupae were kept at 8°C for 135 days and watered once a week, after which they were kept at 20°C. With this latter temperature regime adults emerged within 75 days.

Life history of Salassa daxuensis *Brechlin, 2015*

Two host plants were used, viz. *C. sinensis*, *J. regia*.

Eggs were obtained from wild adult females caught in China: Bifeng Gorge, Ya'an City, Sichuan Province, 1000 m a.s.l., 26-VI-2022.

Eggs white, oblate (fig. 6A). L1 larva similar to *S. mesosa* (fig. 6B). L2 larva also similar to *S. mesosa* but without a black dot on the midline (fig. 6C). L3 and L4 larvae similar to L2 larva, with the same colour pattern and similar head (fig. 6D, E). Head of L5 and L6 larvae rounded, body colour as in L4 larva (fig. 6F, G). Colour of L6 larva changes from green to reddish brown when fully matured before pupation (fig. 6G). Pupae brownish black, darker at high humidity, yellowish brown at low humidity (fig. 6H). Adult morphology see original description (fig. 6I).

Eggs kept at 20°C, hatched within 20 days. Hatching process and larval behaviour similar to *S. shuyiae*. Survival rate was ca. 35% with *J. regia* as host plant and larvae pupated within 45 days, while survival rate was 10% with *C. sinensis* and larvae pupated within 100 days. We also tried *Phellodendron amurense* but larvae remained smaller on this host plant and died in the L5 stage. Pupae were kept at 8°C for 120 days and watered once a week, after which they were kept at 18°C. With this latter temperature regime adults emerged within 75 days.

Life history of Salassa arianae *Brechlin & Kitching, 2010*

Host plant: *Juglans regia*.

Eggs were obtained from wild adult females caught in China: Ningshan County, Ankang City, Shaanxi Province, 1500 m a.s.l., 16-VI-2021.

Eggs white, oblate (fig. 7A). L1 larva similar to *S. mesosa* (fig. 7B). L2 larva similar to *S. mesosa*, but can be recognised by the head with a relatively blunt apex, body midline with two anterior black dots, and abdominal segments III–VI with paired dark dots posteriorly near midline (fig. 7C). L3 and L4 larvae similar to L2 larva, with the same colour pattern; head shaped as an equilateral triangle

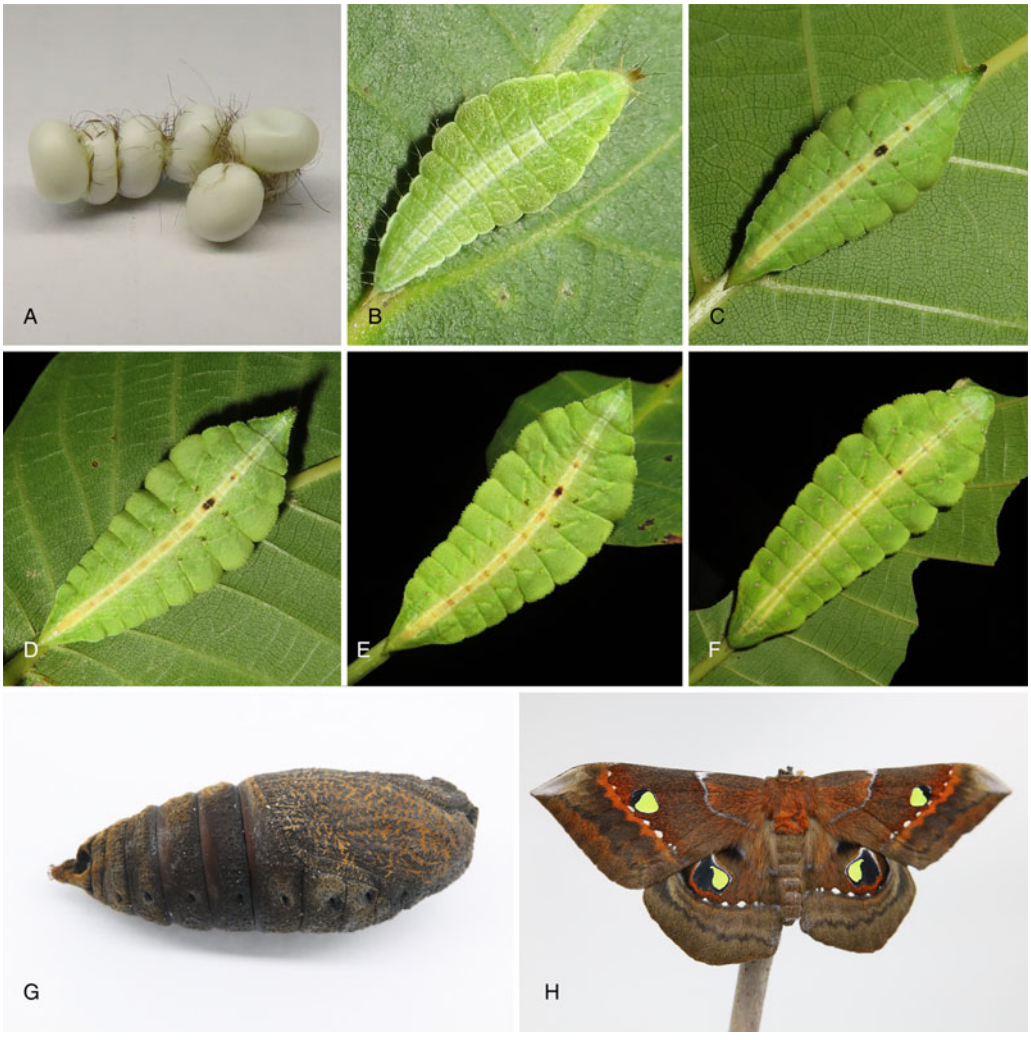

Figure 7. Life history of *Salassa arianae*. (**A**) eggs. (**B**) L1 larva. (**C**) L2 larva. (**D**) L3 larva. (**E**) L4 larva. (**F**) L5 larva. (**G**) pupa. (**H**) female adult.

https://doi.org/10.1017/S0007485323000676 Published online by Cambridge University Press

(fig. 7D, E). Colour pattern of L5 larva similar to L4 larva; head of L5 larva rounded. Larval body colour changes from green to reddish brown when fully matured before pupation (fig. 7F). Pupae brownish black, darker at high humidity, yellowish brown at low humidity (fig. 7G). Adult morphology see original description (fig. 7H).

Eggs kept at 20°C, hatched within 16 days. Hatching process and larval behaviour similar to *S. shuyiae*. Survival rate was ca. 40% until pupation, within 80 days. Pupae were kept at 2–4°C for 120 days and watered once a week, after which they were kept at 18°C. With this latter temperature regime adults emerged within 75 days.

Mitogenome structure of Aglia *and* Salassa

The circular complete mitogenome sequences of *A. homora*, *A. tau*, *S. shuyiae* and *S. mesosa* were 15,354 bp, 15,334 bp, 15,290 bp and 15,289 bp long respectively (fig. 8A–D). These mitogenome sizes are comparable to those of other Saturniidae (Table 1). All of them have 37 genes, including 13 protein-coding genes (PCGs), 22 tRNA genes and two rRNA genes (12S and 16S), with a large non-coding region known as the control region (CR) between *s-rRNA* and *trnM*. Nine PCGs and 14 tRNAs are located on the majority strand (H-strand), while the remaining 14 genes are encoded on the minority strand (L-strand) (Table 2). The four new mitogenomes have the typical gene content and arrangement of most Lepidoptera including Saturniidae (Table 2), with the gene order *trnM-trnI-trnQ*, which is the only difference from the ancestral gene order of insects viz. *trnI-trnQ-trnM* (Cao *et al.*, 2012).

Four PCGs (*ND1*, *ND4*, *ND4L*, and *ND5*) in the four new mitogenomes are not located on the H-strand, but on the

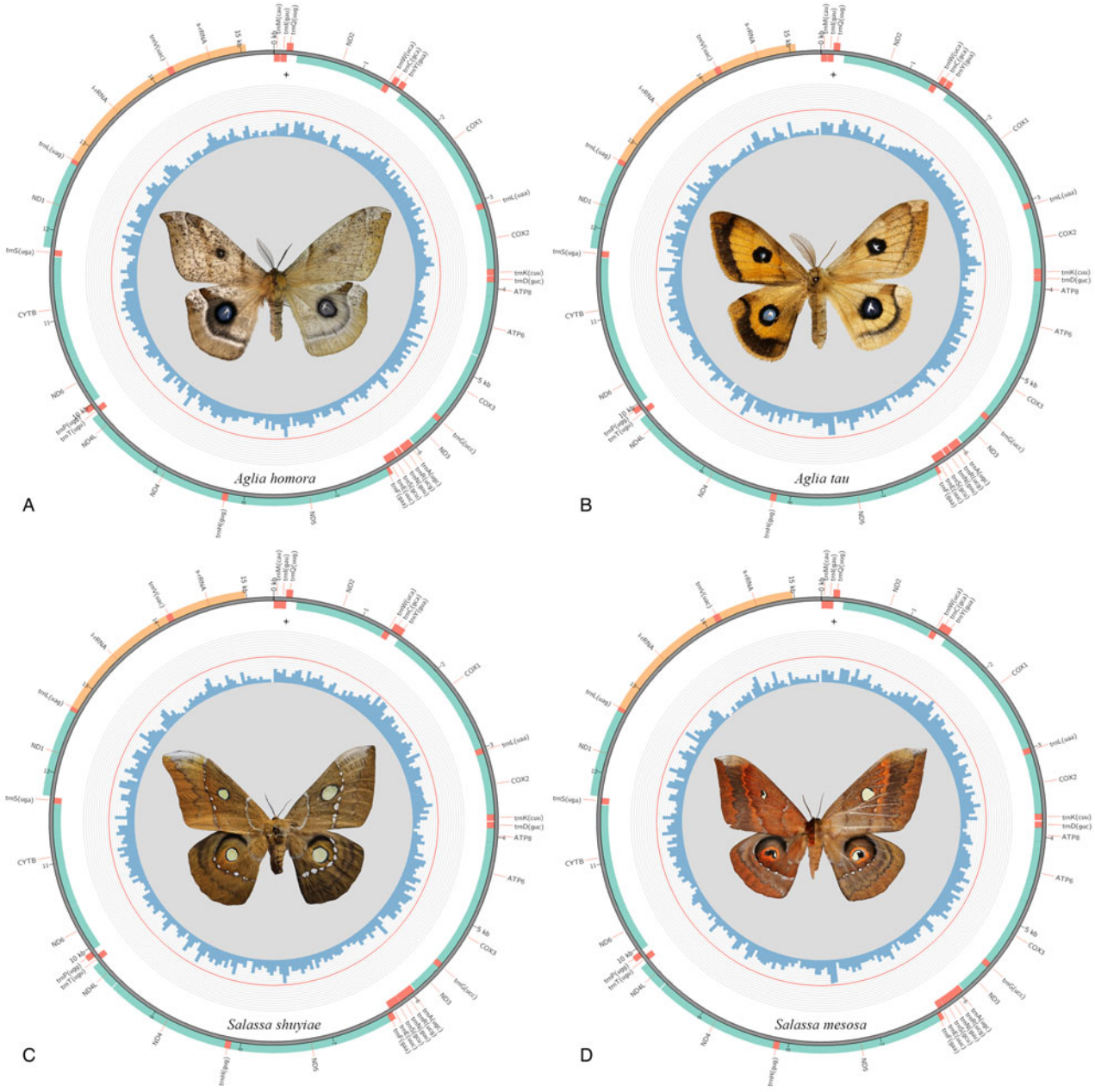

Figure 8. Mitochondrial maps of four species. (**A**) *Aglia homora*. (**B**) *Aglia tau*. (**C**) *Salassa shuyiae*. (**D**) *Salassa mesosa*.

https://doi.org/10.1017/S0007485323000676 Published online by Cambridge University Press

Table 2. Features of the mitogenomes of four saturniid species

		Gene position			
Gene	Strand	*Aglia homora*	*Aglia tau*	*Salassa shuyiae*	*Salassa mesosa*
trnM	J	1–65	1–65	1–70	1–67
trnI	J	77–141	75–139	72–137	67–131
trnQ	N	139–207	137–205	135–203	129–197
ND2	J	259–1272	261–1274	257–1270	246–1259
trnW	J	1280–1346	1282–1348	1279–1346	1268–1336
trnC	N	1339–1401	1341–1403	1339–1402	1329–1391
trnY	N	1424–1488	1416–1480	1403–1465	1392–1455
COI	J	1501–3036	1492–3027	1469–3004	1459–2994
$trnL_2$	J	3032–3098	3023–3089	3000–3065	2990–3055
COII	J	3099–3780	3090–3771	3066–3747	3056–3737
trnK	J	3781–3851	3772–3842	3748–3818	3738–3808
trnD	J	3861–3928	3847–3914	3832–3902	3825–3893
ATP8	J	3929–4093	3915–4079	3903–4067	3894–4058
ATP6	J	4087–4764	4073–4750	4061–4738	4052–4729
COIII	J	4780–5568	4754–5542	4738–5526	4729–5517
trnG	J	5571–5636	5545–5611	5529–5594	5520–5586
ND3	J	5637–5990	5612–5965	5595–5948	5587–5940
trnA	J	6007–6072	5984–6049	5960–6029	5952–6020
trnR	J	6072–6137	6049–6112	6029–6092	6020–6083
trnN	J	6151–6216	6127–6192	6093–6157	6084–6149
$trnS_1$	J	6231–6297	6207–6273	6161–6229	6150–6217
trnE	J	6298–6363	6274–6339	6232–6298	6223–6278
trnF	N	6362–6426	6338–6402	6297–6362	6288–6351
ND5	N	6437–8173	6403–8149	6362–8106	6351–8095
trnH	N	8174–8238	8150–8213	8107–8171	8096–8161
ND4	N	8240–9580	8215–9555	8171–9511	8162–9502
ND4L	N	9581–9871	9557–9847	9523–9810	9516–9806
trnT	J	9879–9942	9856–9919	9826–9889	9823–9887
trnP	N	9943–10,008	9920–9985	9890–9953	9888–9951
ND6	J	10,016–10,549	9993–10,526	9961–10,491	9958–10,494
CYTB	J	10,553–11,704	10,530–11,681	10,498–11,655	10,494–11,645
$trnS_2$	J	11,721–11,785	11,694–11,758	11,663–11,727	11,660–11,725
ND1	N	11,808–12,746	11,781–12,719	11,746–12,684	11,744–12,682
$trnL_1$	N	12,748–12,815	12,721–12,788	12,686–12,753	12,684–12,751
rrnL	N	12,854–14,158	12,813–14,126	12,790–14,082	12,781–14,075
trnV	N	14,182–14,248	14,162–14,228	14,116–14,182	14,109–14,175
rrnS	N	14,249–15,014	14,229–14,994	14,183–14,958	14,176–14,951

L-strand, which is consistent with other saturniid mitogenomes (Table 2) (Chen *et al.*, 2014, 2022). All PCGs start with conventional initiation codons ATN (ATG, ATT, ATA, and ATC), as in other saturniid species, except for the *COI* genes which start with CGA (Table 3). All the PCGs are terminated by typical TAN codons, i.e. TAG for *ND1* and *ND2* of *S. mesosa*, and TAA for all the other PCGs (Table 3).

The four mitogenomes contained 22 typical tRNA genes, whose sizes ranged from 56 bp (*trnE* of *S. mesosa*) to 71 bp (*trnD* of *S. mesosa* and *trnK* of *A. tau, A. homora, S. shuyiae*

https://doi.org/10.1017/S0007485323000676 Published online by Cambridge University Press

Table 3. Initiation codon - termination codon of PCGs and anticodons of tRNAs of the mitogenomes of four saturniid species

		Gene position			
Gene	Strand	*Aglia homora*	*Aglia tau*	*Salassa shuyiae*	*Salassa mesosa*
trnM	J	CAT	CAT	CAT	CAT
trnI	J	GAT	GAT	GAT	GAT
trnQ	N	TTG	TTG	TTG	TTG
ND2	J	ATT-TAA	ATT-TAA	ATC-TAA	ATC-TAG
trnW	J	TCA	TCA	TCA	TCA
trnC	N	GCA	GCA	GCA	GCA
trnY	N	GTA	GTA	GTA	GTA
COI	J	CGA-TAA	CGA-TAA	CGA-TAA	CGA-TAA
$trnL_2$	J	TAA	TAA	TAA	TAA
COII	J	ATT-T	ATT-T	ATG-T	GTG-T
trnK	J	CTT	CTT	CTT	CTT
trnD	J	GTC	GTC	GTC	GTC
ATP8	J	ATT-TAA	ATT-TAA	ATT-TAA	ATT-TAA
ATP6	J	ATG-TAA	ATG-TAA	ATG-TAA	ATG-TAA
COIII	J	ATG-TAA	ATG-TAA	ATG-TAA	ATG-TAA
trnG	J	TCC	TCC	TCC	TCC
ND3	J	ATC-TAA	ATC-TAA	ATT-TAA	ATT-TAA
trnA	J	TGC	TGC	TGC	TGC
trnR	J	TCG	TCG	TCG	TCG
trnN	J	GTT	GTT	GTT	GTT
$trnS_1$	J	GCT	GCT	GCT	GCT
trnE	J	TTC	TTC	TTC	TTC
trnF	N	GAA	GAA	GAA	GAA
ND5	N	ATT-T	ATT-T	ATT-TA	ATA-TA
trnH	N	GTG	GTG	GTG	GTG
ND4	N	ATG-TAA	ATG-TAA	ATG-TAA	ATG-TAA
ND4L	N	ATG-TAA	ATG-TAA	ATG-TAA	ATG-TAA
trnT	J	TGT	TGT	TGT	TGT
trnP	N	TGG	TGG	TGG	TGG
ND6	J	ATA-TAA	ATA-TAA	ATC-TAA	ATT-TAA
CYTB	J	ATG-TAA	ATG-TAA	ATG-TAA	ATG-TAA
$trnS_2$	J	TGA	TGA	TGA	TGA
ND1	N	ATG-TAA	ATG-TAA	ATG-TAA	ATG-TAG
$trnL_1$	N	TAG	TAG	TAG	TAG
rrnL	N	\	\	\	\
trnV	N	TAC	TAC	TAC	TAC
rrnS	N	\	\	\	\

and *S. mesosa*) (Table 2). The secondary structures of the tRNA genes could be folded into the typical clover-leaf structure except for *trnS1* in the four species and *trnE* in *S. mesosa* (fig. 9A–D) whose T-arm were replaced by a loop. This peculiar structure of *trnS1* is commonly found in other saturniid mitogenomes (Lu *et al.*, 2022), but for *trnE* it was never reported before. The size of the CR between *s-rRNA* and *trnM* ranged from 332 bp (*S. mesosa*) to 340 bp (*A. homora* and *A. tau*) (Table 2).

https://doi.org/10.1017/S0007485323000676 Published online by Cambridge University Press

Figure 9. Putative secondary structure of trnE. (**A**) *Aglia homora*. (**B**) *Aglia tau*. (**C**) *Salassa shuyiae*. (**D**) *Salassa mesosa*.

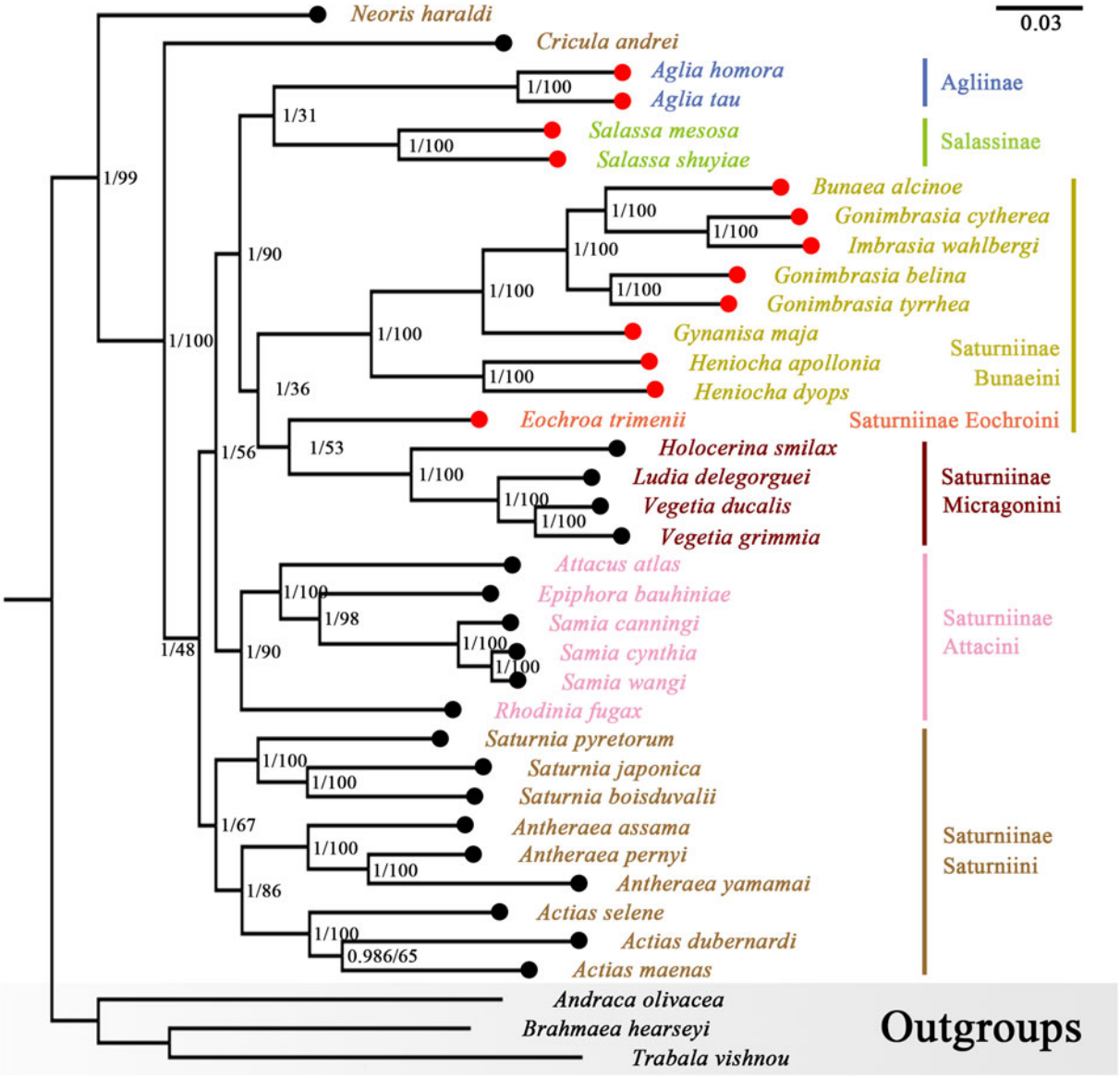

Figure 10. Phylogenetic relationships of Saturniidae constructed by BI and ML methods based on DNA sequences of 13 mitogenomic PCGs. Posterior probability and bootstrap values on node are separated by a slash, red dots represent non-cocooning species, black dots represent cocooning species.

https://doi.org/10.1017/S0007485323000676 Published online by Cambridge University Press

Phylogenetic analysis

Most previous phylogenetic studies of Saturniidae were based on morphological characters or protein coding sequences (Friedlander *et al.*, 1998; Regier *et al.*, 2008; Rubinoff and Doorenweerd, 2020). Regier *et al.* (2008) reconstructed the phylogenetic tree of Saturniidae using four protein coding genes viz. CAD, DDC, period and wingless. Their system is up to now the most commonly used with Agliinae and Salasinae as two monogeneric subfamilies, and Salassinae as sister group of Saturniinae. In this system, the 18 genera used in this study except *Salassa* and *Aglia* belong to the Saturniinae.

The present phylogenetic analysis is based on the 13 PCGs of the four new mitogenomes and the mitogenomes of all the saturniid genera available in GenBank (last visit on April 4, 2023) (Table 1). Three mitogenomes were selected for those genera for which more than three mitogenomes were available (Table 1). In total, the ingroup comprised 34 species from 20 genera, while the outgroup consisted of three species from three different families (fig. 10, Table 1). The resulting BI and ML trees had the same topology as shown in fig. 10 in which: (1) *Neoris haraldi* and *Cricula andrei* appear as single branches with sister group positions to all other ingroup taxa; (2) all these other ingroup taxa form a clade in which the Saturniini of the Saturniinae (including *Actias*, *Antheraea,* and *Saturnia*) consititute a well-supported subclade that is sister to a subclade comprising the other tribes of the Saturniinae along with the Agliinae and Salassinae (fig. 10). Yet these two subclades are only well-supported by BI, not by ML; (3) Within the non-Saturniini subclade, three further clades could be distinguished: one is the Attacini of the Saturniinae (including *Attacus*, *Epiphora*, *Samia* and *Rhodinia*), the second is the Agliinae + Salassinae, and finally the Bunaeini + Eochroini + Micragonini (fig. 10). Yet, only the Attacini clade was well-supported by both BI and ML, the two other clades were only well-supported by BI, not by ML. Hence, in contrast to previous studies (Friedlander *et al.*, 1998; Regier *et al.*, 2008; Rubinoff and Doorenweerd, 2020; Nethavhani *et al.*, 2022), the present results do not support the monophyly of Saturniinae since the Agliinae and Salassinae were placed among the Saturniinae tribes (fig. 10). The most striking result of this work is the placement of *Neoris haraldi* and *Cricula andrei*, since both these species were formerly included in the Saturniini

Figure 11. Pupation behaviours of *Salassa* and *Aglia* species. (**A**) *Salassa shuyiae* larva making pupal chamber. (**B**) *Salassa shuyiae* larva making pupal chamber. (**C**) pupa and pupal chamber of *Salassa shuyiae*. (**D**) *Salassa mesosa* larva making pupal chamber. (**E**) *Salassa mesosa* larva making pupal chamber. (**F**) *Salassa mesosa* pupa inside pupal chamber. (**G**) *Aglia homora* larva making pupal chamber. (**H**) *Aglia homora* larva making pupal chamber. (**I**) *Aglia homora* pupa inside pupal chamber.

https://doi.org/10.1017/S0007485323000676 Published online by Cambridge University Press

of the Saturniinae (Regier *et al.*, 2008; Rubinoff and Doorenweerd, 2020), whereas in the current analyses they are with strong support widely separated from the Saturniini (fig. 10).

Discussion

Pupation behaviour of Aglia *and* Salassa

The five *Salassa* species reared in this study shared a similar pupation process (fig. 11A–F). The day before the larvae fully mature, their food intake decreases. Then the dorsal vessel mid-line becomes brown. Subsequently, a large amount of viscous excreta is discharged from their intestines, while the body colour changes from green to reddish brown (fig. 3G). After this colour transition, larvae spit out liquid from their mouth and spread it all over their body before they descend from trees to pupate in ground surface deposits (fig. 11A–F). The function of the liquid is unknown, but we speculate that it may protect the body during long-distance crawling. Larvae showed, indeed, strong crawling ability and can crawl far away from their host plant. Larvae do not dig into the soil, but look for cracks or press a shallow pit in surface deposits to create a space, after which they spin and pull the surrounding deposits to construct a pupal chamber (fig. 11A–F). They produce only a small amount of silk that does not form a closed cocoon (fig. 11A–F).

The pupation behaviour of *A. tau* and *A. homora* was similar to that of the *Salassa* species, except for some morphological differences (fig. 11G–I). Mature larvae eat less, change from green to red, empty their body, cover their body with a liquid spit from their mouth, descend from their host plant and pupate in the ground (fig. 11G). In contrast to the overground pupation of *Salassa*, the two *Aglia* species pupated underground. Larvae burrowed 2–3 cm into the soil, reinforced their burrow slightly with a small amount of silk and then pupated inside it (fig. 11G–I). This behavioural difference is facilitated by particular morphological features of the *Aglia* larvae and pupae: *Aglia* pupae have multiple tiny spines on their abdominal segments, which can help them to move more efficiently within the soil (figs 2G, 4G). Mature larvae of *Aglia* are densely covered with white tubercles, making their body rough and apt for digging, in contrast to the smooth and soft larvae of *Salassa* (figs 3G, 11G).

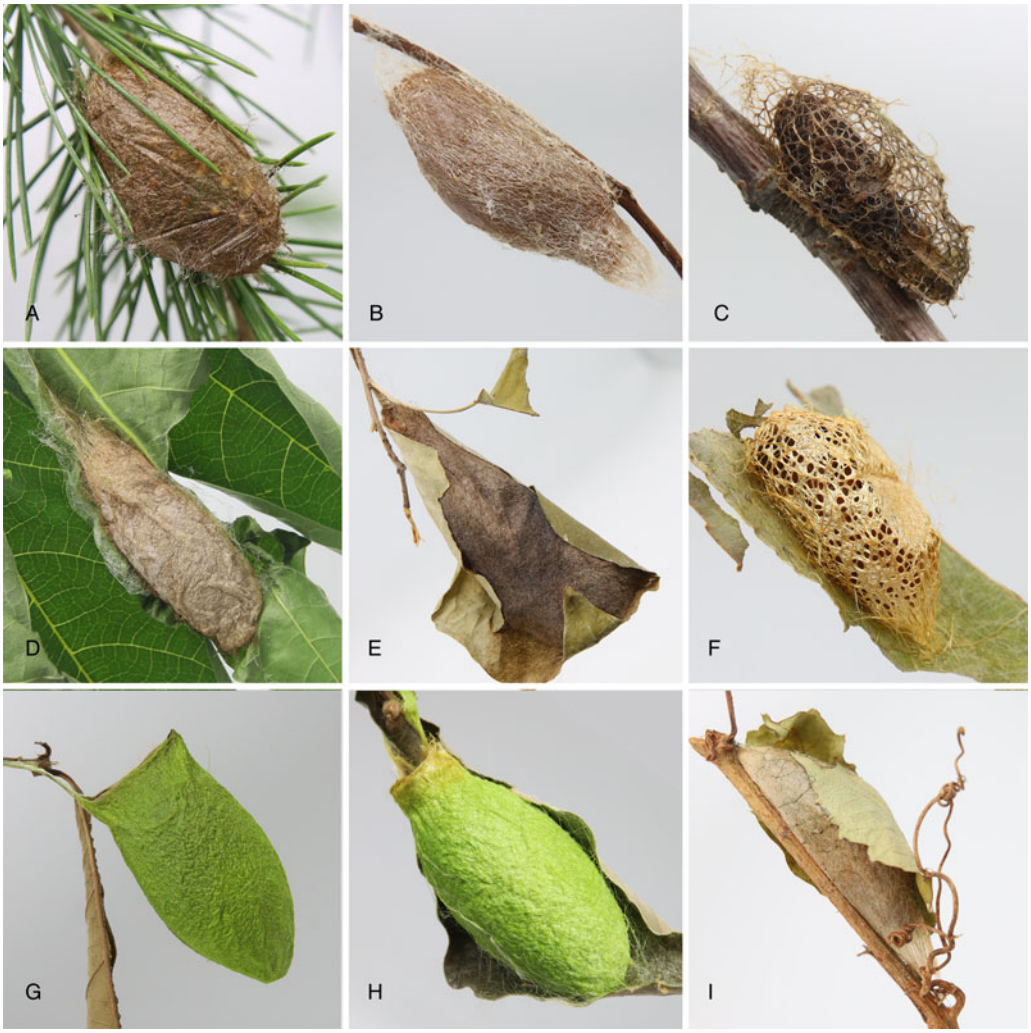

Figure 12. Cocoons of several saturniid genera. (**A**) cocoon of *Actias chrisbrechlinae*. (**B**) cocoon of *Saturnia pyretorum*. (**C**) cocoon of *Saturnia lesoudieri*. (**D**) cocoon of *Samia canningi*. (**E**) cocoon of *Attacus atlas*. (**F**) cocoon of *Cricula trifenestrata*. (**G**) cocoon of *Rhodinia fugax*. (**H**) cocoon of *Antheraea yamamai*. (**I**) cocoon of *Loepa diffundata*.

https://doi.org/10.1017/S0007485323000676 Published online by Cambridge University Press

Loss of cocooning behaviour in Saturniidae

As a common behaviour of Saturniidae and superfamily Bombycoidea, cocooning ought to be an ancestral behaviour of the Saturniidae (Craig, 2003). As such, cocoon morphology and silk composition are highly variable between genera and species (Lampe, 2010) (fig. 12A–I).

Most of the non-cocooning saturniid genera occur in Africa (Lampe, 2010) and of the 10 African genera with mitogenome sequences in GenBank, six are non-cocooning (fig. 10). In Asia, however, only *Aglia* and *Salassa* show non-cocooning behaviour, as we confirm in the present study (fig. 11).

Given that not all Saturniidae show cocooning behaviour and that cocooning is supposed to be an ancestral feature, one may wonder whether the loss of cocooning behaviour evolved once or several times in the Saturniidae. According to Regier *et al.* (2008) Salassinae and Agliinae are unrelated, implying that cocooning behaviour was lost at least twice within the Saturniidae. Moreover, a third loss of cocooning behaviour may be associated with the Bunaeini. However, the present analysis suggests that the three non-cocooning taxa form a clade with the Eochroini and Micragonini (fig. 10). This implies that cocooning behaviour may have been lost only once in the common ancestor of the clade comprising *Salassa* + *Aglia* + Bunaeini + Eochroini + Micragonini, and was secondarily regained in the Micragonini. Yet, the taxon sampling in this study is still far too limited to present this alternative suggestion as well-corroborated and definitive. Hence a more comprehensive phylogenetic analysis is needed to resolve this issue and to further explore the puzzling phylogenetic placements of *Neoris*, *Cricula*, *Salassa* and *Aglia* proposed by the present work.

Acknowledgements. We would like to express our sincere gratitude to Mr. Zhenbang Xu, Shiyu Tong, Haolin Gan and Yangyang Gou for providing eggs and specimens for this study, Mr. Da Pan and Zhiteng Chen for their assistance in phylogenetic analysis.

Financial support. This work is funded by the National Natural Science Foundation of China (31750002, 32070475) and the Priority Academic Program Development of Jiangsu Higher Education Institutions (PAPD).

Competing interests. None.

References

Bernt M, Donath A, Juhling F, Externbrink F, Florentz C, Fritzsch G, Putz J, Middendorf M and Stadler PF (2013) MITOS: improved de novo metazoan mitochondrial genome annotation. *Molecular Phylogenetics and Evolution* **69**, 313–319.

Cao YQ, Ma C, Chen JY and Yang DR (2012) The complete mitochondrial genomes of two ghost moths, *Thitarodes renzhiensis* and *Thitarodes yunnanensis*: the ancestral gene arrangement in Lepidoptera. *BMC Genomics* **13**, 1–13.

Chen F, Porter D and Vollrath F (2012) Morphology and structure of silkworm cocoons. *Materials Science and Engineering: C* **32**, 772–778.

Chen MM, Li Y, Chen M, Wang H, Li Q, Xia RX, Zeng CY, Li YP, Liu YQ and Qin L (2014) Complete mitochondrial genome of the atlas moth, *Attacus atlas* (Lepidoptera: Saturniidae) and the phylogenetic relationship of Saturniidae species. *Gene* **545**, 95–101.

Chen S, Zhou Y, Chen Y and Gu J (2018) fastp: an ultra-fast all-in-one FASTQ preprocessor. *Bioinformatics (Oxford, England)* **34**, i884–i890.

Chen DB, Zhang RS, Jin XD, Yang J, Li P and Liu YQ (2022) First complete mitochondrial genome of *Rhodinia* species (Lepidoptera: Saturniidae): genome description and phylogenetic implication. *Bulletin of Entomological Research* **112**, 243–252.

Craig CL (2003) *Spiderwebs and Silk: Tracing Evolution From Molecules to Genes to Phenotypes*. New York, USA: Oxford University Press, 230 pp.

Eltayba MT and Magidb TDA (2013) Relation between female cocoons (pupae) measurements and the number of eggs laid (fecundity) by the wild silk moth *Epiphora bauhiniae* (Gurin-meneville) Lepidopetera: saturniidae. *International Journal of Advance Industrial Engineering* **1**, 16–19.

Folmer O, Black M, Hoeh W, Lutz R and Vrijenhoek R (1994) DNA primers for amplification of mitochondrial cytochrome coxidase subunit I from diverse metazoan invertebrates. *Molecular Marine Biology and Biotechnology* **3**, 294–299.

Friedlander TP, Horst KR, Regier JC, Mitter C, Peigler RS and Fang QQ (1998) Two nuclear genes yield concordant relationships within Attacini (Lepidoptera: Saturniidae). *Molecular Phylogenetics and Evolution* **9**, 131–140.

Friedlander TP, Peigler RS, Regier JC and Mitter C (2002) Monophyly, composition, and relationships within Saturniinae (Lepidoptera: Saturniidae): evidence from two nuclear genes. *Insect Systematics & Evolution* **33**, 9–21.

Kalyaanamoorthy S, Minh BQ, Wong TKF, von Haeseler A and Jermiin LS (2017) ModelFinder: fast model selection for accurate phylogenetic estimates. *Nature Methods* **14**, 587–589.

Katoh K and Standley DM (2013) MAFFT multiple sequence alignment software version 7: improvements in performance and usability. *Molecular Biology and Evolution* **30**, 772–780.

Kim JS, Kim MJ, Jeong JS and Kim I (2018) Complete mitochondrial genome of *Saturnia jonasii* (Lepidoptera: Saturniidae): genomic comparisons and phylogenetic inference among Bombycoidea. *Genomics* **110**, 274–282.

Kimura M (1980) A simple method for estimating evolutionary rate of base substitutions through comparative studies of nucleotide sequences. *Journal of Molecular Evolution* **16**, 111–120.

Lampe RE (2010) *Saturniidae of the World. Their Life Stages From the Eggs to the Adults*. Munich, Germany: Verlag Dr Friedrich Pfeil, 368 pp.

Li W, Zhang Z, Lin L and Terenius O (2017) *Antheraea pernyi* (Lepidoptera: Saturniidae) and its importance in sericulture, food consumption, and traditional Chinese medicine. *Journal of Economic Entomology* **110**, 1404–1411.

Liu Z and Peigler RS (2021) The life history and entomophagy of *Saturnia centralis* and related Saturniidae. *The Journal of the Lepidopterists' Society* **75**, 174–186.

Lowe TM and Chan PP (2016) tRNAscan-SE On-line: integrating search and context for analysis of transfer RNA genes. *Nucleic Acids Research* **44**, 54–57.

Lu D, Huang Y, Naumann S, Kitching IJ, Xu Z, Sun Y and Wang X (2022) Mitochondrial genomes of two wild silkmoths, *Samia watsoni* and *Samia wangi* (Lepidoptera: Saturniidae), and their phylogenetic implications. *European Journal of Entomology* **119**, 337–353.

Meng G, Li Y, Yang C and Liu S (2019) MitoZ: a toolkit for mitochondrial genome assembly, annotation and visualization. *Nucleic Acids Research* **47**, e63.

Miller MA, Wayne P and Terri S (2011) The CIPRES science gateway: A community resource for phylogenetic analyses. p. 1 in Proceedings of the 2011 TeraGrid Conference: Extreme Digital Discovery, Salt Lake City Utah, 18–21 July 2011 1–8 New York, Association for Computing Machinery. https://doi.org/10.1145/2016741.2016785

Naumann S and Lalhmingliani E (2019) Notes on taxa of the *Salassa lemaii* group (Lepidoptera: Saturniidae) with the description of a new species from Mizoram, India. *BIONOTES* **21**, 152–158.

Naumann S, Brosch U and Nässig WA (2003) A catalogue and annotated checklist of the subfamily Agliinae PACKARD, 1893 (Lepidoptera: Saturniidae). 1. Review of the *Aglia* species with description of a new taxon from Sichuan, China. *Nachrichten des Entomologischen Vereins Apollo, Frankfurt am Main, NF* **24**, 173–182.

Nethavhani Z, Straeuli R, Hiscock K, Veldtman R, Morton A, Oberprieler RG and van Asch B (2022) Mitogenomics and phylogenetics of twelve species of African Saturniidae (Lepidoptera). *PeerJ* **10**, e13275.

Oberprieler RG, Morton AS and van Noort S (2021) The life history of *Vegetia grimmia* (Geyer, 1832) (Saturniidae: Bunaeinae: Micragonini), with an account of its discovery, distribution and taxonomic distinction. *Metamorphosis* **32**, 74–92.

Peigler RS and Liu Z (2022) The life history and phylogeny of *Samia watsoni* (Saturniidae), A Relict Species Endemic to China. *The Journal of the Lepidopterists' Society* **76**, 93–101.

https://doi.org/10.1017/S0007485323000676 Published online by Cambridge University Press

Perna NT and Kocher TD (1995) Patterns of nucleotide composition at fourfold degenerate sites of animal mitochondrial genomes. *Journal of Molecular Evolution* **41**, 353–358.

Poulton EB (1888) XV. Notes in 1887 upon lepidopterous larvæ, &c, including a complete account of the life-history of the larvæ of *Sphinx convolvuli* and *Aglia tau*. *Transactions of the Royal Entomological Society of London* **36**, 515–606.

Regier JC, Grant MC, Mitter C, Cook CP, Peigler RS and Rougerie R (2008) Phylogenetic relationships of wild silkmoths (Lepidoptera: Saturniidae) inferred from four protein-coding nuclear genes. *Systematic Entomology* **33**, 219–228.

Ronquist F, Teslenko M, Mark PVD, Ayres DL, Darling A, Höhna S, Larget B, Liu L, Suchard MA and Huelsenbeck JP (2012) MrBayes 3.2: efficient Bayesian phylogenetic inference and model choice across a large model space. *Systematic Biology* **61**, 539–542.

Rougerie R and Estradel Y (2008) Morphology of the preimaginal stages of the African emperor moth *Bunaeopsis licharbas* (Maassen and Weyding): phylogenetically informative characters within the Saturniinae (Lepidoptera: Saturniidae). *Journal of Morphology* **269**, 207–232.

Rozas J, Ferrer-Mata A, Sánchez-DelBarrio JC, Guirao-Rico S, Librado P, Ramos-Onsins SE and Alejandro SG (2017) DnaSP 6: DNA sequence polymorphism analysis of large data sets. *Molecular Biology and Evolution* **34**, 3299–3302.

Rubinoff D and Doorenweerd C (2020) Systematics and biogeography reciprocally illuminate taxonomic revisions in the silkmoth genus *Saturnia* (Lepidoptera: Saturniidae). *The Journal of the Lepidopterists' Society* **74**, 1–6.

Stamatakis A (2014) RAxML version 8: a tool for phylogenetic analysis and post-analysis of large phylogenies. *Bioinformatics (Oxford, England)* **30**, 1312–1313.

Talavera G and Castresana J (2007) Improvement of phylogenies after removing divergent and ambiguously aligned blocks from protein sequence alignments. *Systematic Biology* **56**, 564–577.

Tamura K, Stecher G and Kumar S (2021) MEGA 11: molecular evolutionary genetics analysis version 11. *Molecular Biology and Evolution* **38**, 3022–3027.

Taylor TA (1964) Notes on the biology of *Bunaea alcinoe* Cram. (Lepidoptera: Saturniidae). *Annals and Magazine of Natural History* **7**, 17–25.

Tsukada M, Kajiura Z, Shoumura S and Satoh S (2012) Spinning behaviors and physical properties of silk fiber from the wild silkworm, *Rhodinia fugax*. *Journal of Silk Science and Technology of Japan* **20**, 27–33.

Yanai Z, Sartori M, Dor R and Dorchin N (2017) Molecular phylogeny and morphological analysis resolve a long-standing controversy over generic concepts in Ecdyonurinae mayflies (Ephemeroptera: Heptageniidae). *Systematic Entomology* **42**, 182–193.

Zhang W and Kohll S (2008) *Salassa shuyiae* n. sp., a new giant silkmoth from Hainan, China (Lepidoptera, Saturniidae, Salassinae). *Nachrichten des entomologischen Vereins Apollo N.F* **29**, 47–52.

Zhang X, Yue C, Liu A and Ma P (2011) Research on biological characteristics of *Neoris haraldi* Schawerda. *Xinjiang Agricultural Sciences* **48**, 672–676.

Zhang D, Gao F, Jakovli´c I, Zou H, Zhang J, Li WX and Wang GT (2020) PhyloSuite: an integrated and scalable desktop platform for streamlined molecular sequence data management and evolutionary phylogenetics studies. *Molecular Ecology Resources* **20**, 348–355.

https://doi.org/10.1017/S0007485323000676 Published online by Cambridge University Press